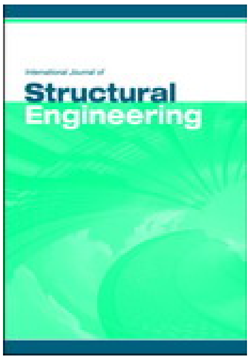

International Journal of Structural Engineering

ISSN online: 1758-7336 - ISSN print: 1758-7328
https://www.inderscience.com/ijstructe

Method for calculating compression resistance of reinforced masonry elements using deformation diagrams

Dzmitry N. Lazovski, Aliaksandr M. Khatkevich, Ellijah Chaparanganda

DOI: 10.1504/IJSTRUCTE.2024.10062428

Article History:

Received:	12 October 2022
Last revised:	29 August 2023
Accepted:	30 August 2023
Published online:	26 February 2024

Method for calculating compression resistance of reinforced masonry elements using deformation diagrams

Dzmitry N. Lazovski

Department of Structural Engineering,
Polotsk State University,
211440, Novopolotsk, Belarus
Email: d.lazovki@psu.by

Aliaksandr M. Khatkevich

Structural Testing and Research Centre,
Polotsk State University,
211440, Novopolotsk, Belarus
Email: a.khatkevich@psu.by

Ellijah Chaparanganda*

Department of Civil and Environmental Engineering,
Botswana International University of Science and Technology
Plot 10071, Boseja, Palapye, Botswana
Email: chaparanganda@biust.ac.bw
*Corresponding author

Abstract: When calculating the compression resistance of reinforced masonry elements, only the final stage before failure is considered. Complete material deformation diagrams and the redistribution of forces between masonry and longitudinal reinforcement in any given cross-section are not considered. Therefore, the purpose of this study is to develop a methodology to calculate the compression resistance of reinforced masonry elements that considers the physical nonlinear deformation of unreinforced and masonry with transverse reinforcement in horizontal mortar joints and longitudinal steel reinforcement, which will allow obtaining deformation parameters at any loading stage. Calculation algorithms for compression resistance and deformation of masonry elements at any loading stage are presented. The used experimental studies of the most characteristic reinforced masonry elements were selected studies published in open access sources. Verification of the proposed calculation methodology was performed and showed a good convergence of the theoretical and experimental values of load-bearing capacity and deformability.

Keywords: physical nonlinearity; reinforced masonry element; material deformation diagram approach; elastoplastic work; uniaxial stress state; idealised parabolic-line diagrams; nonlinear parabolic deformation diagrams; compressive resistance.

Reference to this paper should be made as follows: Lazovski, D.N., Khatkevich, A.M. and Chaparanganda, E. (2024) 'Method for calculating compression resistance of reinforced masonry elements using deformation diagrams', *Int. J. Structural Engineering*, Vol. 14, No. 1, pp.42–62.

Biographical notes: Dzmitry N. Lazovski earned his DSc in Structural Engineering from the Belarussian State Academy in 1999. He is a Professor of Structural Engineering working with the Department of Structural Engineering at Polotsk State University, Novopolotsk, Belarus. His research interests are in structural health and monitoring of civil and industrial infrastructure, and structural engineering (theory, materials, and design).

Aliaksandr M. Khatkevich earned his PhD in Structural Engineering from Brest State Technical University in 2021. He is working as the Head of the Structural Engineering Department as well as a Research Engineer of the Testing and Research Center of Polotsk State University, Novopolotsk, Belarus. His research interests are in masonry structures, structural analysis of existing structures, strengthening, restoration, and rehabilitation of existing building structures.

Ellijah Chaparanganda earned his PhD in Structural Engineering from the Belarussian State Academy in 1999. He is working as a Lecturer in Structural Engineering at the Department of Civil and Environmental Engineering of Botswana International University of Science and Technology, Palapye, Botswana. His research interests are in masonry structures, structural analysis of existing structures, strengthening, restoration, and rehabilitation of existing building structures.

1 Introduction

Reinforced masonry elements are made by placing reinforcing longitudinal steel rods perpendicular to the horizontal mortar joints of the masonry, and by placing transverse mesh reinforcements in plane of the horizontal mortar joints. The combination of reinforcement and masonry elements increases the compression and bending resistance, which is reflected in their articulation effect in the multilayer masonry walls of the load-bearing elements of the building structures.

The role and use of reinforcement will continue to increase as it allows the creation of structural systems with the required load-bearing capacity, continuity, and plastic deformability. This is vital as it protects buildings structures from progressive collapse and increases seismic resistance. In addition, the reinforcement of the masonry also makes it possible to increase the resistance of structures to shock and explosive loads. In this regard, there is a need to conduct more research such as that conducted for reinforced concrete and unreinforced masonry structures (Akid et al., 2021; Anas et al., 2021a, 2021b, 2022, 2023a, 2023b; Sun et al. 2023; Wang et al. 2023).

It is well known that masonry is a heterogeneous structure consisting of masonry units laid on mortar in a certain order. The strength and deformation properties of the masonry are anisotropic. The masonry units and mortar experience a complex state of stress caused by the sharp difference in the properties of the masonry units and mortar and interaction at the joints, uneven local deformations of the mortar bed, bending and shearing of masonry units, and the presence of vertical joints. There are various research works aimed at micro-modelling in which brickwork is considered as discrete material (Abdulla et al., 2017; Addessi et al., 2014; Angelillo et al., 2014; Bagi and Angelillo, 2023; EN 1990; Mohammad et al., 2015; Sousa et al., 2015). It should be noted that to date, discrete models are not widely used in engineering practice due to the relatively high complexity of calculations, the large amount of initial data in the form of finite elements and the complexity of describing the contact zone between masonry units and mortars. Discrete models are typically for research purposes only.

Reinforced masonry structures are massive structures with large cross-sections. These massive structures are subject to a simple stress state of compression or bending. This simple state of stress makes it possible to apply an idealised calculation model by replacing the inhomogeneous structure of the masonry with a homogeneous medium with averaged physical and mechanical properties that can be considered in a calculation model in the form of material deformation diagrams.

Furthermore, it is particularly important that the hypothesis of plane sections (Bernoulli hypothesis) is applied to the distribution of the relative deformations ($\varepsilon_z = f(x, y)$) of the cross-sections along the length of both unreinforced and reinforced masonry structures with several rows of masonry units. Several experimental studies (Figarov, 1957; Kameyko, 1939, 1949, 1950; Lazovsky and Khatkevich, 2019; Pildish and Polyakov, 1955; Polyakov et al., 1973) on compressed unreinforced and reinforced elements with rectangular and T-shaped cross-sections confirmed, with sufficient practical accuracy, the applicability of this hypothesis, the results of which are incorporated into design standards (Eurocode 6, 1995; SP 15.13330.2012, 2012; SP 5.02.01-2021, 2021; TKP 45-5.02-308-2017 (33020), 2018).

According to Eurocode 6 (1995), TKP 45-5.02-308-2017 (33020) (2018), SP 5.02.01 (2021), the compression resistance of reinforced masonry elements is calculated based on the following conditions:

- Maintaining the flatness of the cross-sections (Bernoulli hypothesis).
- The relative deformation values of both the reinforcement and the adjacent masonry elements are the same. That is, the connection of the longitudinal steel reinforcement and the masonry elements is guaranteed.
- The tensile strength of the masonry perpendicular to the horizontal joints is not considered.
- The masonry deformation diagram can be parabolic, parabolic-linear, or rectangular.
- During compression, the ultimate relative deformations value of the masonry depends on the type of masonry. Therefore, the ultimate relative deformation value of the most compressed masonry edge of the section (ultimate compressibility ε_{mu}) does not exceed 3.5% for group 1 masonry units and 2.0% for group 2 masonry units.
- According to TKP EN 1992-1-1-2009* (0250) (2015) and SP 5.03.01-2020 (2022), the deformation diagram of steel reinforcement and its ultimate deformations ε_{sy} are assigned based on the type of reinforcing steel.
- When using hollow blocks or arranging niches in which longitudinal steel reinforcement is installed, the deformation characteristics of concrete for filling the voids are considered to be the same as the characteristics of masonry.

- The calculated compressive strength value in cases where masonry and concrete for filling voids of the compressed cross-sectional zone, is considered to be that of a transformed section of the less durable material.
- The distribution of the calculated compressive stress diagram for masonry or concrete used for filling voids has a rectangular shape.

A design model [Eurocode 6, 1995; TKP 45-5.02-308-2017 (33020), 2018; SP 5.02.01-2021, 2021] of a reinforced masonry element cross-section of width *b* with longitudinal reinforcement area A_s is presented in Figure 1.

Figure 1 Design diagram of the cross-section of a bending and (or) compressed reinforced masonry element, (a) cross-section (b) deformation diagram (c) compressive stresses diagram and scheme of design forces (see online version for colours)

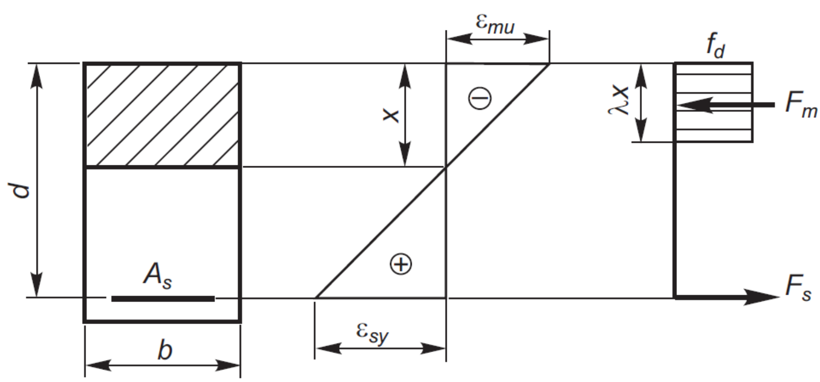

Notes: x – the distance from the neutral axis to the most compressed edge; λ_x – nominal height of the compressed zone; $F_s = f_{yd}$ x A_s – tensile force in the reinforcement; $F_m = f_d \times b \times \lambda_x$ – resultant compressive force in masonry for the rectangular stress diagram; f_d and f_{yd} calculated compressive strength of masonry or concrete filling in the direction of the acting longitudinal forces and longitudinal steel reinforcement, respectively.

Source: SP 5.02.01-2021 (2021, p.58)

Despite the calculation conditions prescribed above, the design standards do not provide any specific conditions for their implementation. At the ultimate stage of loading, the compressive resistance values, N_u of short reinforced masonry elements are calculated using the method of sections which is based on the use of the equilibrium equations of internal and external forces, without taking into account the curvilinear strain diagrams [Eurocode 6, 1995; SP 15.13330.2012, 2012; SP 5.02.01-2021, 2021; TKP 45-5.02-308-2017 (33020), 2018]. When calculating the theoretical compression resistance value N_{Rdu}, it is hypothesised that the longitudinal reinforcement and the masonry will attain the ultimate design values of strength, f_d and f_{yd}, respectively before failure, while the transverse reinforcement is considered for the increased values of the compressive strength of the masonry. Therefore, at the ultimate stage, the curvilinear stress diagram of the compressed cross-sectional zone, Figure 2(a), is replaced by a shortened rectangular diagram, Figures 2(b) and 2(c).

Figure 2 Distribution of stresses in the cross-section, (a) actual (b) per SP 15.13330.2012 (2012) (c) per Eurocode 6 (1995), TKP 45-5.02-308-20170(33020) (2018), SP 5.02.01-2021 (2021) (d) considering elastoplastic work per Belentsov (2001)

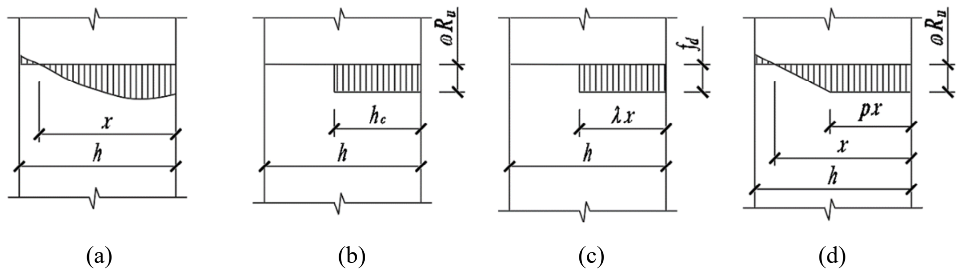

Notes: h – The height of the section of the eccentricity plane, x – the height of the compressed cross-sectional zone, h_c – height of the compressed cross-sectional area per SP 15.13330.2012 (2012), λ_x and f_d – same as in Figure 1, p – the plasticity number, R_u – Tensile strength of masonry per SP 15.13330.2012 (2012), w – a coefficient that considers the magnitude of the eccentricity (SP 15.13330.2012, 2012)

Belentsov (2001) attempted to take into account the physical nonlinearity of the masonry material. He proposed a model based on the elastoplastic work in which the relationship between stresses and deformations is linear; in the cross-section, part of the compressed zone is in the plastic state while the other part is in the elastic state; and the normal stresses σ diagram of the compressed zone has a trapezoidal shape. In addition, this calculation method does not take into account the full diagram of masonry deformations, and its practical application is complicated by the multiplicity of the value of the plasticity number 'p' as shown in Figure 2(d).

As the analysis showed, there is currently no clearly defined method for calculating the compressive resistance of short-reinforced masonry elements, which includes the calculation of the stress-strain state parameters in each loading stage, taking into account the physical nonlinearity of the masonry and reinforcement. The known calculation methods take into account the resistance only in the ultimate stage, and do not take into account either the nonlinearity of material deformations or the redistribution of forces in the cross-sections of the reinforced masonry elements.

Therefore, the aim of this study is to develop a method for calculating the compressive resistance of short-reinforced masonry elements, which takes into account the physical nonlinearity of the deformation of materials in the form of unreinforced masonry, masonry with transverse reinforcement in horizontal mortar joints and longitudinal steel reinforcement, and which allows to obtain the parameters of the stress-strain state of compressed elements at any loading stage. To achieve this goal, the following tasks were performed:

- To take as generalised characteristics of the mechanical properties of materials, the relationship between normal stresses and relative deformations ($\sigma = f(\varepsilon_z)$) in the form of deformation diagrams of unreinforced masonry, masonry with transverse reinforcement in horizontal mortar joints, longitudinal steel reinforcement.
- To formulate equations and algorithms for the calculation of the parameters of the stress-strain state of short-reinforced masonry elements at all loading stages.

- To verify the calculation method by comparing the theoretical values of the compression resistance at the ultimate stage of short-reinforced masonry elements and the stress-strain state parameters at intermediate loading stages, with the corresponding experimental values from the selected research works.

2 Deformation diagrams

2.1 Masonry deformation diagrams

A complete '$\sigma - \varepsilon$' deformation diagram of the unreinforced masonry under uniaxial stress state and the action of longitudinal compressive forces perpendicular to the horizontal mortar joints is presented as a curvilinear dependence (Akhaveissy, 2012; Hendry, 1998; Kaushik, 2007a; 2007b; Mohammad et al., 2007; Stavridis and Shing, 2010). This deformation diagram is characterised by base points under compression (ε_{m1}; f_m) and under tension (ε_{t1}; f_t) separating the ascending and descending branches with the angle of inclination φ of the diagram, which depends on the elastic properties of the masonry (modulus of elasticity E_m), as shown in Figure 3.

There are several known approximations of masonry deformation diagrams in compression. Logarithmic dependencies (Mohamad et al., 2007; Mohammad et al., 2012; SNiP II-22-81) are known to have a good agreement with the experimental data, but they do not describe the descending branch of the diagram. Akhaveissy (2012), Hendry (1998), and Kaushik et al. (2007a, 2007b) noted that it is possible to approximate the deformation diagram of unreinforced masonry by parabolic dependence, which are traditionally used to describe the diagram of heavy concrete. Using the same dependencies '$\sigma - \varepsilon$' for concrete and masonry is quite common since their properties are close. This approach was used by Dajun et al. (1998), Stavridis and Shing (2010), and Yaremenko and Yaremenko (2016) in their research work.

Figure 3 Complete diagram of masonry deformation (see online version for colours)

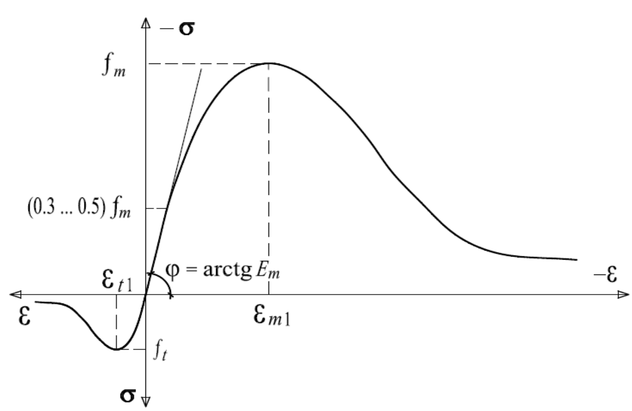

The design standards, Eurocode 6 (1995), SP 5.02.01-2021 (2021), TKP 45-5.02-308-2017 (3302) (2018) do not contain an analytical description of the diagram of deformation of unreinforced masonry under compression, but they only give its graphical representation. The distribution of the non-decreasing branch of the actual parabolic diagram (pos. 1, Figure 4) of the deformation and the horizontal section of the idealised parabolic-line diagrams (pos. 2 and 3, Figure 4) is limited by the value of ε_{mu} (the geometrical parameters of test specimens are determined according to EN 1052-1:1998). There are no approximations of masonry deformation diagrams with transverse reinforcement in horizontal mortar joints in the regulatory and technical literature.

Figure 4 Diagrams of masonry deformation under axial short-term compression according to TKP 45-5.02-308-2017 (33020) (2018) and SP 5.02.01-2021 (2021)

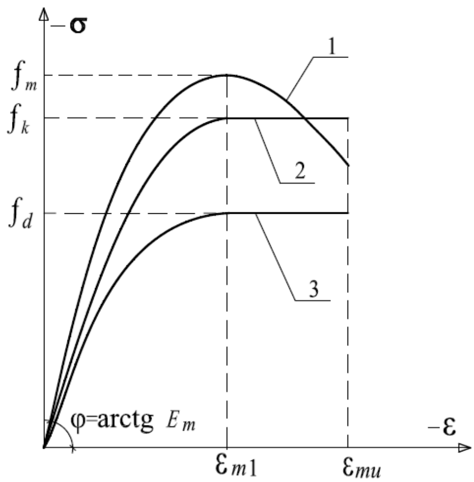

Notes: 1 – parabolic; 2 – idealised parabolic-linear; 3 – calculated parabolic-linear

Figure 5 Diagrams of deformation '$\sigma - \varepsilon$' of masonry material, (a) diagram of unreinforced masonry (b) diagram of masonry with transverse reinforcement in horizontal mortar joints (see online version for colours)

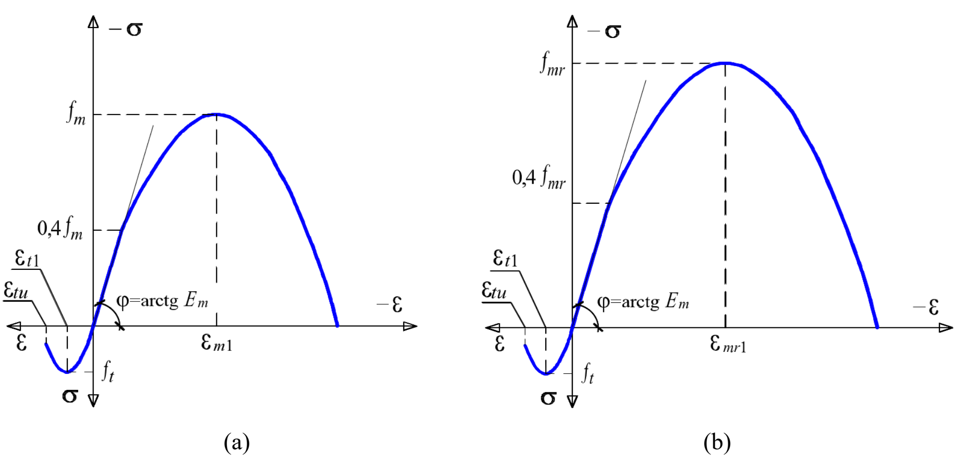

Data on the tensile strain diagram of the masonry and the corresponding strength f_t can be found in the literature in a very limited extent. There is also no single standardised method for obtaining the tensile characteristics of masonry. Akhaveissy (2012) provided information on the tensile deformation diagram of masonry in the form of a bilinear graph. Mohammad et al. (2012) gave a description of the tensile diagram in which the ascending branch is represented by a linear dependence, and the descending branch is represented by an exponential function.

The authors of this article propose to use the nonlinear parabolic deformation diagrams '$\sigma - \varepsilon$' from Figure 5 to account for the physical nonlinearity of materials of unreinforced masonry and transversely reinforced masonry in horizontal mesh-type mortar joints within the framework of the proposed method for calculating the compression resistance of reinforced stone elements. The tensile section of the diagram will show the redistribution of forces in the eccentrically compressed reinforced masonry elements and perform crack resistance calculations.

The approximations of the deformation diagrams of Figure 5 are represented by parabolic dependences:

$$\begin{cases} \sigma = \left(2\dfrac{\varepsilon}{\varepsilon_{m1}} - \left(\dfrac{\varepsilon}{\varepsilon_{m1}}\right)^2\right) f_m \\ \sigma = \left(2\dfrac{\varepsilon}{\varepsilon_{mr1}} - \left(\dfrac{\varepsilon}{\varepsilon_{mr1}}\right)^2\right) f_{mr} \\ \sigma = \left(2\dfrac{\varepsilon}{\varepsilon_{t1}} - \left(\dfrac{\varepsilon}{\varepsilon_{t1}}\right)^2\right) f_t \end{cases} \tag{1}$$

where

- ε_{m1}, ε_{mr1} and ε_{t1} are the relative deformations corresponding to the stresses f_m, f_{mr} and f_t (MPa) respectively.
- f_m and f_t (MPa) are ordinates of the absolute maximum stresses in the deformation diagrams of unreinforced masonry under axial compression and tension, respectively.
- f_{mr} (MPa) is the ordinate of the maximum stresses in the deformation diagram of masonry with transverse reinforcement in horizontal mortar joints in the form of wire mesh under axial compression.

In the absence of experimental data, the ordinate f_m of the material deformation diagram is computed by the formula:

$$f_{mr} = f_m + \frac{K\mu f_y}{100} \tag{2}$$

where

- K is the coefficient of efficiency of the transverse reinforcement. The recommended value of the coefficient is $K = 2$.
- μ is the percentage of reinforcement. It is determined by the ratio of the volume of mesh wire reinforcement in horizontal mortar joints to the percentage volume of the reinforced masonry element.
- f_y is the yield strength of the reinforcement used to produce the transverse reinforcement meshes.

In the absence of experimental data, it is proposed to calculate the ordinate f_t of the deformation diagram for materials of unreinforced masonry and masonry with transverse reinforcement in horizontal mortar joints as follows.

$$f_t = 0.1 f_m \tag{3}$$

The relative deformation $\varepsilon_t 1$ corresponding to the maximum stresses f_t in axial tension and ultimate relative deformations ε_{tu} is given by:

$$\begin{cases} \varepsilon_{t1} = f_t / E_m \\ \varepsilon_{tu} = 2\varepsilon_{t1} \end{cases} \tag{4}$$

where E_m (MPa) is the modulus of elasticity of masonry elements.

2.2 *Diagrams of deformation of longitudinal steel reinforcement*

The deformation diagram of the reinforcement '$\sigma_s - \varepsilon_s$' has a curvilinear relationship, which is characterised by the base points and an angle of inclination tangential to the diagram and depends on the elastic properties of the material. Therefore, when calculating elements of building structures, the compression and tensile strain sections of the material diagrams are traditionally considered to be the same.

Due to the presence of elastic, elastoplastic and plastic stages of deformation, the mathematical description of the experimental '$\sigma_s - \varepsilon_s$' curves quite a challenging task. However, several mathematical relationships are known that approximate curved diagrams of rebar reinforcement (Karpenko et al., 2016; Madatyan, 2000).

Figure 6 Deformation diagram of longitudinal steel reinforcement

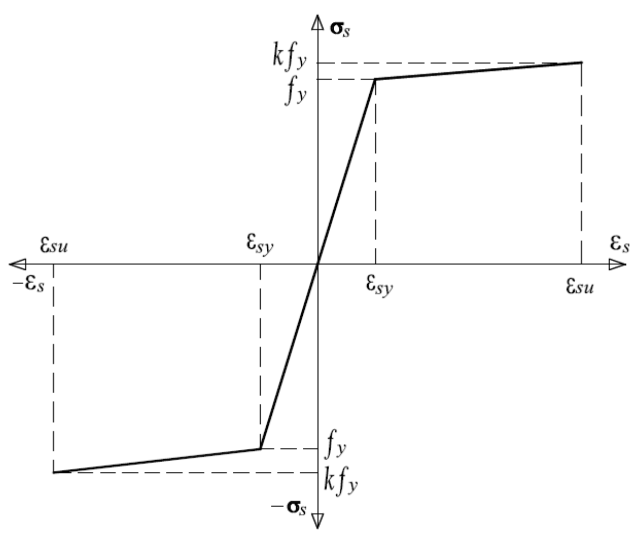

Experience in the calculation of reinforced concrete elements have shown that the use of accurate analytical relationships '$\sigma_s - \varepsilon_s$' of the deformation diagrams of reinforcement complicates the process of calculating the stress-strain state and significantly affects the accuracy of the calculated values of compression resistance (bending) (Bleshchik et al., 2003). In this regard, it is advisable to use simplified segmented linear dependencies passing through the main base points to approximate the deformation diagram of longitudinal steel reinforcement.

As per the deformation diagrams, the strength properties of 'hard' steel are not fully utilised, resulting in the use of 'soft' steel with a physical yield strength as longitudinal steel reinforcement for short, reinforced masonry elements. Therefore, the deformation diagram of the longitudinal steel reinforcement is as assumed to be that of an ideal elastoplastic body (Prandtl diagram) with limited yield area (Figure 6), which allows to consider the physical nonlinearity of the longitudinal steel reinforcement within the framework of the development and testing of the proposed methodology for calculating the compression resistance of short, reinforced masonry elements.

The deformation criterion for strength (failure) in the form of ultimate relative deformations of the reinforcement ε_u, is widely used in the calculation of structural elements. The provisions of Eurocode 6 (1995), SP 5.02.01-2021 (2021); TKP 45.0308-2017 (33020) (2018) for the calculation of compressed reinforced masonry elements, prescribes to consider the characteristics of the longitudinal steel reinforcement according to the design standards for reinforced concrete structures [TKP EN 1992-1-1-2009* (0250), 2015; SP 5.03.01-2020, 2022] whilst limiting the relative deformations to $\varepsilon_{su} = \pm$ 10%.

For the calculation of the compressive resistance of short-reinforced masonry elements, it is proposed:

- To take f_y (MPa) as the average value of the stresses corresponding to the yield strength of the reinforcement.
- To determine the deformation ε_{sy} as the ratio of the yield strength of the reinforcement f_y to its modulus of elasticity E_s.
- To consider the complete redistribution of forces in the cross-section of the reinforced masonry elements, with a recommended extra margin of ε_{su} = 20%.

3 Method for calculating the compression resistance of reinforced masonry elements

Prerequisites and assumptions:

- The cross-section of the reinforced masonry element can consist of various materials in any combination. So, the cross-section can be composed of unreinforced masonry, masonry with transverse reinforcement in horizontal mortar joints, longitudinal steel reinforcement, which in turn can be placed freely in concrete mortar outside the masonry or in special niches (grooves).
- Unreinforced masonry and masonry with transverse reinforcement in horizontal mortar joints should be considered as homogeneous continuum material with averaged physical and mechanical characteristics presented in the form of material deformation diagrams.
- Under load, special structural design measures during the installation of the reinforced masonry elements ensure that the longitudinal steel reinforcement of the reinforced masonry elements works jointly in all deformation stages. Material

deformation diagrams of longitudinal steel reinforcement reflect their physical and mechanical characteristics.

- The calculation cross-section of the reinforced masonry element should be considered as a set of elementary areas (layers) within which the stresses are uniformly distributed and correspond to the mean value of the stresses at the boundaries of the areas (layers). Research shows that in the calculation of reinforced concrete elements, the dimensions of the areas (layers) should not exceed 1/10 of the cross-sectional size (Bleshchik et al., 2003).
- Each elemental area (layer) of the cross-section experiences either compression or tension.
- The distribution of the relative deformations ε_z over the cross-section of the reinforced masonry element should be assumed to be linear according to the condition of the flat-layered cross-sectional hypothesis.

Figure 7 Design model of a short, reinforced stone element, (a) design cross-section under simple eccentric compression ($e_y > 0$, $e_x = 0$) (b) distribution of relative deformations ε_z over the cross-section (c) distribution of normal stresses over the cross-sections (d) the design cross-section for the general case of eccentric compression ($e_y > 0$, $e_x > 0$)

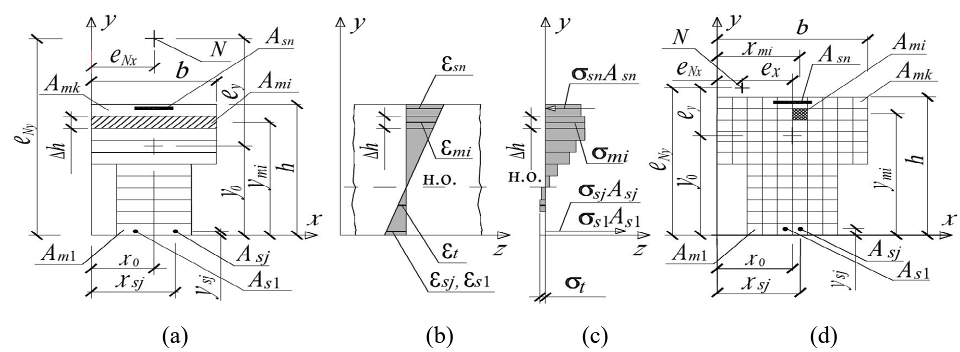

The cross-section of the reinforced masonry element should be divided into k elementary layers of height $\Delta h = h/k$ with the cross-sectional area of the i^{th} elementary layer A_{mi}, as shown in Figure 7(a). The cross-section contains n bars of longitudinal steel reinforcement, where the cross-sectional area of the j^{th} bar is A_{sj}.

Distribution of relative deformations ε_z of the cross-section of the reinforced masonry element in consideration of the accepted prerequisites, the distribution of the relative deformations ε_z over the cross-section of the reinforced masonry element is linear according to the hypothesis of flat sections. Then, for the i^{th} elementary area and the j^{th} longitudinal steel rod reinforcement:

$$\begin{cases} \varepsilon_{mi} = \dfrac{1}{r_y}\left(y_{mi} - y_0\right) + \dfrac{1}{r_x}\left(x_{mi} - x_0\right) + \varepsilon_N \\ \varepsilon_{sj} = \dfrac{1}{r_y}\left(y_{sj} - y_0\right) + \dfrac{1}{r_x}\left(x_{sj} - x_0\right) + \varepsilon_N \end{cases} \tag{5}$$

where

- ε_{mi}, ε_{sj} are the relative deformations in the i^{th} elementary area and the j^{th} longitudinal steel reinforcement rod, respectively.
- $1/r_y$, $1/r_x$ are curvatures in the planes of y and x axes, respectively.
- y_{mi}, x_{mi} are the coordinates of the centre of gravity of the i^{th} elementary area (layer).
- y_0, x_0 are the coordinates of the centre of gravity of the calculated cross-section.
- ε_N is the relative compressive strain caused by the longitudinal force N.
- y_{sj}, x_j are coordinates of the j^{th} longitudinal steel reinforcement bar.

Each elemental area (layer) and longitudinal steel reinforcement bar experiences compression or tension. At each level of loading, the stress in the elementary masonry areas, σ_{mi} and the longitudinal steel reinforcement bars σ_{sj} are related to the relative strains ε_{mi}, ε_{sj} due to the secant strain moduli $E_{mi}^{/}, E_{sj}^{/}$ of the masonry works and the longitudinal steel reinforcement, as given by the following equation:

$$\begin{cases} \sigma_{mi} = f\left(\varepsilon_{mi}\right) = E_{mi}^{/}\varepsilon_{mi} \\ \sigma_{sj} = f\left(\varepsilon_{sj}\right) = E_{sj}^{/}\varepsilon_{sj} \end{cases} \tag{6}$$

The conditions of distribution of relative strains (stress-strain relationships) on the flat-layer sections are determined by solving the following equations for the general case of eccentric compression applying the equilibrium equations.

$$\begin{aligned} &\varepsilon_N\left(\sum_{i=1}^{k} E_{mi}^{/}A_{mi} + \sum_{j=1}^{n} E_{sj}^{/}A_{sj}\right) + \frac{1}{r_x}\left(\sum_{i=1}^{k} E_{mi}^{/}A_{mi}\left(x_{mi}-x_0\right) + \sum_{j=1}^{n} E_{sj}^{/}A_{sj}\left(x_{sj}-x_0\right)\right) \\ &+\frac{1}{r_y}\left(\sum_{i=1}^{k} E_{mi}^{/}A_{mi}\left(y_{mi}-y_0\right) + \sum_{j=1}^{m} E_{sj}^{/}A_{sj}\left(y_{sj}-y_0\right) - N = 0\right) \end{aligned} \tag{7}$$

$$\begin{aligned} &\varepsilon_N\left(\sum_{i=1}^{k} E_{mi}^{/}A_{mi}\left(x_{mi}-x_0\right) + \sum_{j}^{n} E_{sj}^{/}A_{sj}\left(x_{sj}-x_0\right)\right) + \frac{1}{r_x}\left(\begin{array}{c} \sum_{j=1}^{k} E_{mi}^{/}A_{mi}\left(x_{mi}-x_0\right)^2 \\ +\sum_{j=1}^{n} E_{sj}^{/}A_{sj}\left(x_{sj}-x_0\right)^2 \end{array}\right) \\ &+\frac{1}{r_y}\left(\sum_{i=1}^{k} E_{mi}^{/}A_{mi}\left(y_{mi}-y_0\right)\left(x_{mi}-x_0\right) + \sum_{j=1}^{n} E_{sj}^{/}A_{js}\left(y_{sj}=y_0\right)\left(x_{sj}-x_0\right)\right) - Ne_x = 0 \end{aligned} \tag{8}$$

$$\begin{aligned} &\varepsilon_N\left(\sum_{i=1}^{k} E_{mi}^{/}A_{mi}\left(y_{mi}-y_0\right) + \sum_{j=1}^{n} E_{sj}^{/}A_{sj}\left(y_{sj}-y_0\right)\right) \\ &+\frac{1}{r_x}\left(\sum_{i=1}^{k} E_{mi}^{/}A_{mi}\left(y_{mi}-y_0\right)\left(x_{mi}-x_0\right) + \sum_{j=1}^{n} E_{sj}^{/}A_{sj}\left(x_{sj}-x_0\right)\left(y_{sj}-y_0\right)\right) \\ &+\frac{1}{r_y}\left(\sum_{i=1}^{k} E_{mi}^{/}A_{mi}\left(y_{mi}-y_0\right)^2 + \sum_{j=1}^{n} E_{sj}^{/}A_{sj}\left(y_{sj}-y_0\right)^2\right) + Ne_y = 0 \end{aligned} \tag{9}$$

Figure 8 Algorithm of the method for calculating the compression strength of a short masonry element with simple eccentric compression $\varepsilon_y > 0$, $\varepsilon_x > 0$

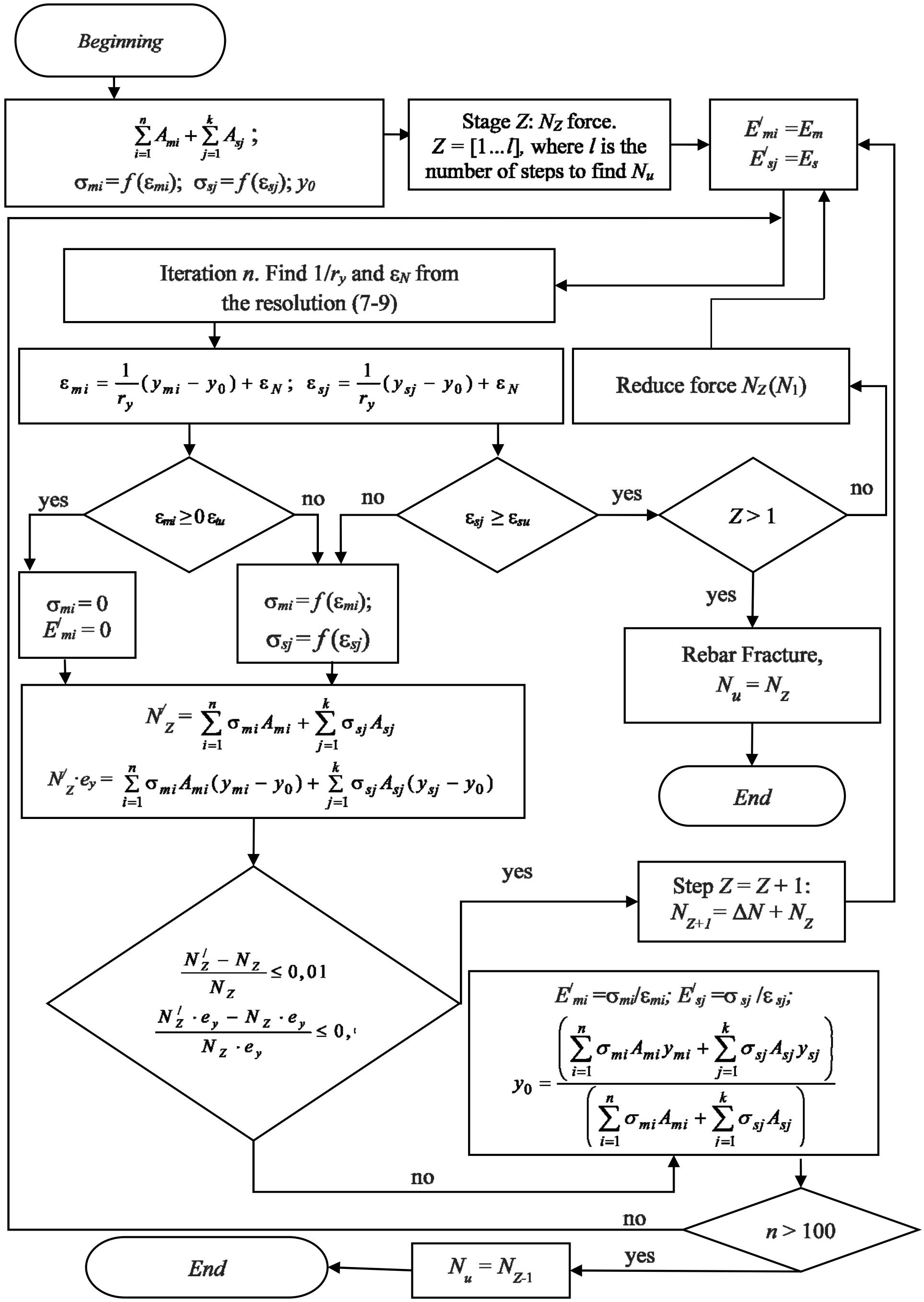

Algorithms for calculating the compressive resistance of short-reinforced masonry elements, including the parameters of their stress-strain state in each loading stage, are implemented using the Beta program (Glukhov and Khatkevich, 2016). The algorithm for calculating the compression resistance of a short-reinforced masonry element using the example of a simple eccentrical (off-centre) compression [Figure 7(a)] is presented in Figure 8.

For reinforced masonry elements, it is proposed to take the value of compression resistance N_u at the ultimate strength stage as the maximum force experienced by the element, based on the condition of compatibility of deformations of the masonry and longitudinal steel reinforcement, in which the volume of the normal stresses diagram reaches its maximum. This approach will make it possible to take into account the redistribution of forces in the cross-section of reinforced masonry elements consisting of materials with different physical and mechanical characteristics and to determine by calculation the ultimate compression deformations ε_{mu} of masonry materials exceeding the normalised values of its ultimate compressibility.

The 'Beta' program, developed at Polotsk State University, allows one to set the strength and deformation characteristics of materials and determine the deformation-based method of calculating cross-sections of reinforced masonry.

4 Verification of the calculation methodology

The verification of the developed calculation method was carried out by comparing:

- Theoretical $N_{u,t}$ values calculated using the proposed method, the values of the compression resistance of short-reinforced masonry elements at the ultimate stage with the corresponding experimental values $N_{u,exp}$ formulated from selected research studies using the procedures of GOST 8462-85 (1985).
- Theoretical and experimental parameters of the stress-strain state in the form of graphs of the deformation of longitudinal steel reinforcement and masonry of the most compressed and tensioned cross-sectional zones of short-reinforced masonry elements formulated from the selected research studies.

The experimental studies were selected based on the tests results carried out on samples of reinforced masonry elements:

- With longitudinal and transverse reinforcement in horizontal mortar joints and combined reinforcement, performed by Kameyko (1939, 1949, 1950) on samples of 1.5 mm × 2 mm and 2 mm × 2 mm brick cross-sections (designated as II – X series) made from artificial masonry units (silicate and ceramic bricks with a bending strength range of 2.23 to 3.59 MPa and a compressive strength range of 11.58 to 14.0 MPa, determined by the method of GOST 8462-85 (1985). A masonry mortar with a composition 1: 0.15: 4 was used in the experiments with Portland cement: lime: sand with an average strength of 6.38 MPa obtained by testing cubes with 70.7 mm edge as per GOST 5802-86 (1992) method, and 1: 3 (Portland cement: sand, of 18.6 MPa average strength). Cement-sand mortar with a composition of 1: 3 and heavy concrete with a compressive strength of 12.3 MPa was used for filling and concreting of the niches in which the longitudinal reinforcement was installed. The longitudinal reinforcement was done using ∅12 mm steel rod reinforcement with a yield strength of f_y = 300 Mpa, ∅16 mm with f_y = 228 MPa, ∅9.7 mm with f_y = 245 MPa, determined according to the PN-70/B-12016 method (1970);

transverse mesh reinforcement made of ∅5 mm wire with f_y = 594 MPa. Longitudinal reinforcement rods were made with bends entering the compressed zone by 15–30 cm and placed in a concrete layer. Stir-ups were placed at the height of every two rows of bricks to avoid a possible loss of stability of the compressed reinforcement and to ensure maximum strength with masonry. The percentage of longitudinal reinforcement varied between 0 to 0.92% and transverse reinforcement between 0 to 1.04%. The reinforcement schemes of experimental samples are shown in Figure 9.

- With longitudinal and transverse reinforcement in horizontal mortar joints on samples made from sawn stone and tested by Figarov (1957) and Pildish and Polyakov (1955) (series designated Fg1 – Fg7). For the preparation of samples, masonry units of size 20×20×40 cm with compressive strength of 4.71 MPa (PN-70/B-12016, 1970) on a complex mortar mix ratio of 1: 0.3: 4 (cement: lime: sand) were used. For longitudinal reinforcement, steel reinforcement of diameter, and yield strength of: ∅11 mm, f_y = 320 MPa, ∅12 mm, f_y = 283 MPa, ∅16mm, f_y = 246 MPa, ∅26 mm, f_y = 360 MPa (PN-EN 1015-11, 2001) were used. Stirrup clamp devices built through one row of masonry were used to provide joint work of masonry and longitudinal reinforcement. Transverse mesh reinforcements were made from ∅6.45 mm wire with yield strength of f_y = 237 MPa. The percentage of longitudinal reinforcement varied from 0 to 0.495%, and transverse from 0 to 1.09%. Reinforcement schemes are shown in Figure 10.
- With transverse reinforcement in horizontal mortar joints on samples made from artificial masonry units (ceramic bricks) tested by Drobiec (2004) (series designated D, E, F) and samples prepared and tested by the authors (series designated CII, CIII, CV, CVI, CVIII) (Lazovsky and Khatkevich, 2019). The strength characteristics of masonry units, mortar, and reinforcement in Drobiec (2004) research studies were considered based on the test results that met the national standards requirements (PN-70/B-12016, 1970; PN-71/B-04500, 1971; PN-91/H-04310, 1991; PN-EN 1015-11:2001, 2001; PN-EN 772-1, 2003). The percentage of transverse reinforcement varied between 0.034% to 0.1%. Meshes and individual steel rods with diameters 1.2 mm, 3.75 mm, 5 mm, and 6 mm were used for the reinforcement.
- The samples of the studies conducted by the authors were made using mortar of a given composition with a compressive strength ranging from 6.85 MPa to 8.95 MPa and solid bricks: for the CII, CIII series, the average compressive strength was 16.7 MPa, with a bending strength of 4.21 MPa; for series CV, CVI, CVIII with an average compressive strength of 24.1 MPa, and bending strength of 3.9 MPa. Testing of masonry and mortar samples was carried out using a hydraulic press according to GOST 5802-86 (1992) and GOST 12004-81 (2011). The cross-sectional reinforcement was provided by wire meshes with 4 mm diameter and yield strength of 509 MPa (PN-70/B-12016, 1970). The percentage of transverse reinforcement in the CII, CIII series was 0.4%, and in the CV, CVI, CVIII series it was 0.2%.

Figure 9 Reinforcement schemes of samples of experiments carried out by Kameyko (1939, 1949, 1950) (see online version for colours)

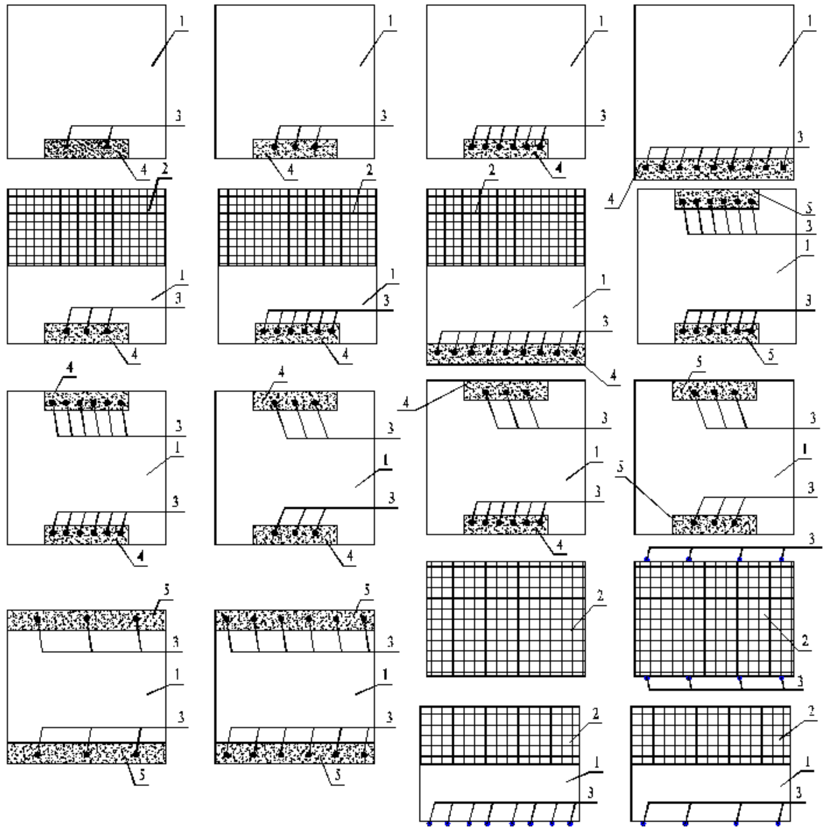

Notes: 1 – masonry; 2 – masonry with transverse reinforcement; 3 – longitudinal reinforcement; 4 – mortar; 5 – concrete

Figure 10 Scheme of reinforcement of experiments samples by Figarov (1957) (see online version for colours)

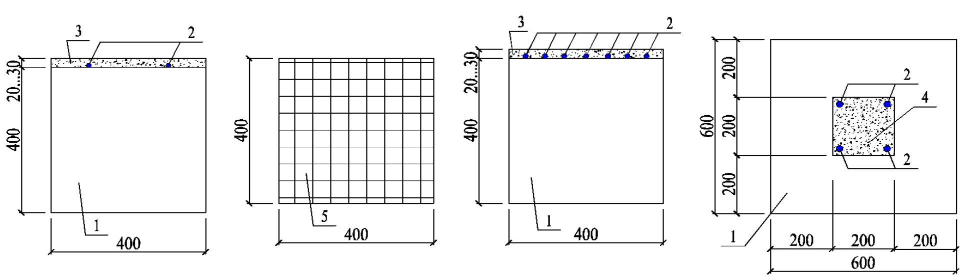

Notes: 1 – masonry; 2 – longitudinal reinforcement; 3 – mortar; 4 – concrete; 5 – masonry with transverse reinforcement

Figure 11 '$N_{u,exp} – N_t$' diagrams, (a) for samples tested by Kameyko (1939, 1949, 1950) (b) for samples tested by Figarov (1957) (c) for samples tested by Drobiec (2004) and authors own tests (see online version for colours)

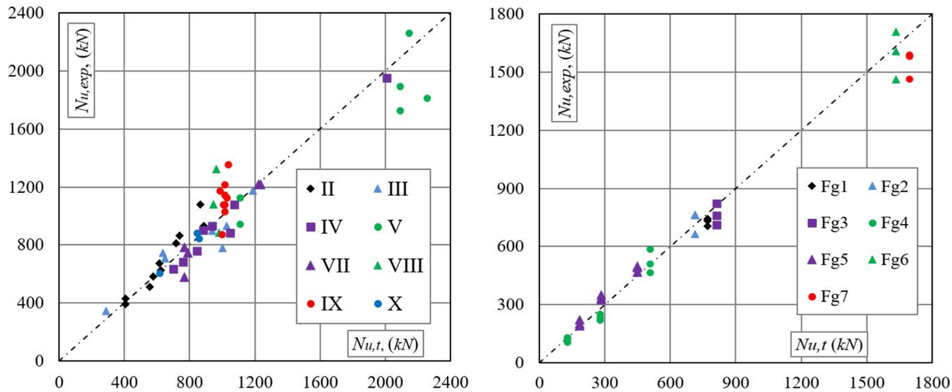

(a) (b)

Source: Lazovsky and Khatkevich (2019)

Figure 11 '$N_{u,exp} – N_t$' diagrams, (a) for samples tested by Kameyko (1939, 1949, 1950) (b) for samples tested by Figarov (1957) (c) for samples tested by Drobiec (2004) and authors own tests (continued) (see online version for colours)

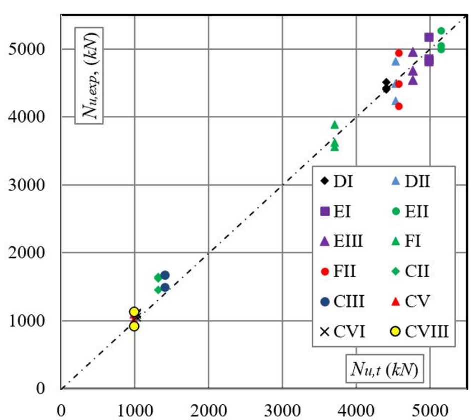

(c)

Source: Lazovsky and Khatkevich (2019)

A good convergence of theoretical $N_{u,t}$ and experimental values of compression resistance at the ultimate stage of loading of short-reinforced stone elements was established:

- According to the results of the sample tests of the research studies conducted by Kameyko (1939, 1949, 1950), the value of the variation coefficient error vector was $V_b = 0.13$ with a direct probabilistic resistance model slope magnitude of $b = 0.98$.
- According to sample tests results 1from Figarov (1957), the value $V_b = 0.11$ with $b = 0.96$.

- According to the sample tests results from Drobiec (2004) and the authors own tests results, the value of $V_b = 0.10$ with $b = 1.02$. '$N_{u,exp} - N_t$' diagrams are given in Figure 11.

Figure 12 '$N - \varepsilon_z$' deformation graphs of longitudinal steel reinforcement of the most compressed and tensioned faces of the most characteristic samples from the selected sample studies (see online version for colours)

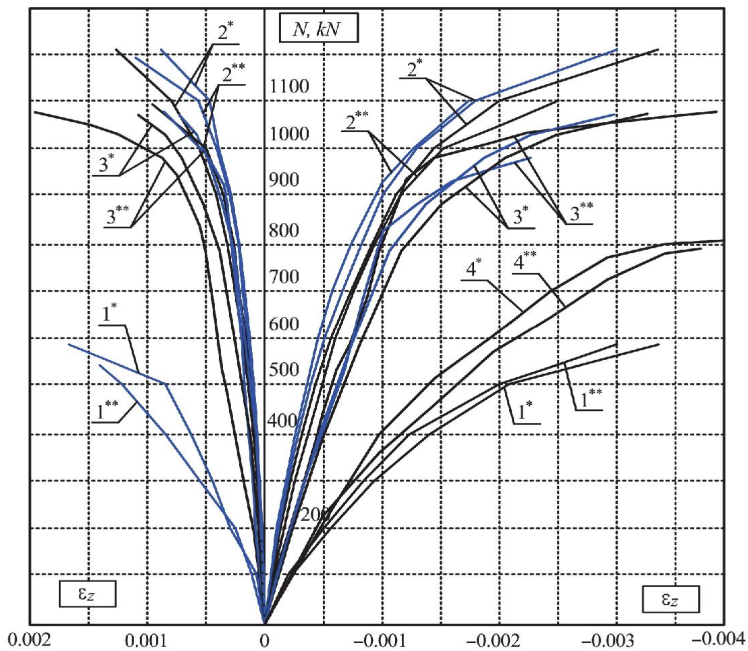

Notes: —— longitudinal steel reinforcement;
—— the most compressed (stretched) face of the cross section.
1 – sample with single longitudinal reinforcement; 2, 3 – samples with double longitudinal reinforcement; 4 – sample with mixed reinforcement; * – according to the developed calculation method; ** – by experimental values

Comparison of what was obtained theoretically with the help of the developed method for calculating the deformation graphs of longitudinal steel reinforcement and masonry of the most compressed and tensioned cross-sectional zones allows us to conclude that the proposed calculation model on the behaviour of the reinforced masonry elements under load is satisfactory.

Figure 12 shows theoretical and experimental graphs of the deformation of the most characteristic short-reinforced masonry elements of the compared research studies.

5 Conclusions

The results of the study show the applicability of the deformation approach to calculate the compression resistance of short-reinforced stone elements. Considering the physical nonlinearity of the deformation of materials makes it possible to obtain, by calculation, parameters of the stress-strain state close to the experimental data. In the future, research in this area should be continued, taking into account the effects of the flexibility of the compressed elements and the duration of the load (the effect of masonry creep), taking into account the work of the reinforced masonry elements strengthened under load.

References

Abdulla, K.F., Cunningham, L.S. and Gillie, M. (2017) 'Simulating masonry wall behaviour using a simplified micro-model approach', *Engineering Structures*, Vol. 151, pp.349–365, DOI:10.1016/j.engstruct.2017.08.021.

Addessi, D. et al. (2014) 'Modeling approaches for masonry structures', *The Open Civil Engineering Journal*, Vol. 8, pp.288–300, DOI:10.2174/1874149501408010288.

Akhaveissy, A.H. (2012) 'The DSC model for the nonlinear analysis of in-plane loaded masonry structures', *The Open Civil Engineering Journal*, Vol. 6, No. 1, pp.200–214.

Akid, A.S.M., Rashid, M.H. and Sobuz, M.H.R. (2021) 'Effect of masonry infill wall with opening on reinforced concrete frame due to seismic loading: parametric study', *International Journal of Structural Engineering*, Vol. 11, No. 1, pp.84–105, DOI:10.1504/IJSTRUCTE.2021.112103.

Anas, S.M., Alam, M. and Umair, M. (2021a) 'Experimental and Numerical Investigations on performance of reinforced concrete slabs under explosive-induced air-blast loading: a state-of-the-art review', *Structures*, Vol. 31, pp.428–461, Elsevier, DOI: 10.1016/j.istruc.2021.01.102.

Anas, S.M., Ansari, M.I. and Alam, M. (2021b) 'A study on existing masonry heritage building to explosive-induced blast loading and its response', *International Journal of Structural Engineering*, Vol. 11, No. 4, pp.387–412, DOI: 10.1504/IJSTRUCTE.2021.118065.

Anas, S.M., Alam, M., Isleem, F.H., Najm, H.M. and Sabri (2022) 'Ultra-high performance concrete (UHPC) and C.FRP tension rebars: a unique combinations of materials for slabs subjected to low velocity drop impact loading', *Frontier Materials, Section Structural Materials*, November, Vol. 9, p.1061297, DOI: 10.3389/fmats.2022.1061297.

Anas, S.M., Alam, M. and Sharig, M. (2023a) 'Damage response of conventionally reinforced two-way spanning concrete slab under eccentric impacting drop weight loading', *Defence Technology*, January, Vol. 19, pp.12–34, Elsevier, DOI: 10.1016/j.dt.2022.04.011.

Anas, S.M., Shariq, M., Alam, M., Ahmed, M., Yosri, A.M. and Mongy, M.A. (2023b) 'Influence of supports on the low velocity impact response of square RC slab of standard concrete and ultra-high performance concrete: FEM-based computational analysis', *Buildings, MDPI*, Vol. 13, No. 5, DOI: 10.3390/buildings13051220.

Angelillo, M., Lourenço P.B. and Milani, G. (2014) 'Masonry behaviour and modelling', in Angelillo, M. (Ed.): *Mechanics of Masonry Structures*, pp.1–26, CISM Intern. Centre for Mech. Sciences, Wien, DOI:10.1007/978-3-7091-1774-31.

Bagi, K. and Angelillo, M. (2023) *Discrete Computational Mechanics of Masonry Structures*, Springer, ISBN: 978-3-031-32476-5, 609pp., DOI:10.1007/978-3-031-32476-5.

Belentsov, Y. (2001) *Reinforcement of Stone Walls and Walls, Considering the Elastoplastic Work of Masonry of Reconstructed Residential Buildings*, 23 May, author. dis. ... Cand. techn. Sciences, St. Petersburg State University bulletin, – SPb, 24pp.

Bleshchik, N.P. et al. (Ed.) (2003) in Petsolda, T.M. and Tura, V.V. (Eds.): *Reinforced Concrete Structures: The Fundamentals of Theory, Calculation, and Construction*, Brest State Technical University, 379pp.

Building Mortars (1992) *Test Methods: GOST 5802-86. Replacing GOST 5802-78; Introduced. 01.07.86*, Vol. 22, Moscow Publishing House of Standards, Moscow.

Dajun, D., Xishao, L. and Juan, Z. (1988) 'Experimental research on strength of brick masonry reinforced with new type of transverse reinforcement', *Journal of Building Structures*, Vol. 9, No. 1, pp.53–58.

Drobiec, Ł. (2004) *Analysis of Solid Brick Walls with Reinforcement in Supporting Welds Subjected to Vertical Loads*, pr. PhD / Ł. Drobiec. – Gliwice: [s. n.], 183pp.

EN (1990) *Eurocode 0: Basis of Structural Design*.

EN 1052-1 (1998) *Methods of Test for Masonry – Part 1: Determination of Compressive Strength*.

Eurocode 2 (2015) *Design of Reinforced Concrete Structures, Part 1-1: General Rules and Regulations for Buildings*, ТКП EN 1992-1-1-2009* (0250), Introduced, 01.01.10, Minsk: Ministry of Architecture and Construction, Belarus, XIV, 205p.

Eurocode 6 (1995) *Design of Masonry Structures, Part 1-1: Rules for Reinforced and Unreinforced Masonry*, ENV 1996-1-1.

Figarov, A.G. (1957) 'Strength and elastic properties of non-reinforced and reinforced masonry from limestone stone dust of the Ashperon', in Onishchik, L.I. (Ed.): *Research on Stone Constructions: State Academy: Building and Architecture of the USSR*, pp.248–268, Center for Scientific Research Institute of Building Constructions, Moscow.

Glukhov, D.O. and Khatkevich, A.M. (2016) 'Method for calculating the strength of compressed stone elements in cross-sections, normal to the longitudinal axis', *Applied Sciences*, Vol. 8, pp.73–79, Vestnik Polotsk State University, Series F, Construction, Novopolotsk, Belarus.

Hendry, A.W. (1998) *Structural Masonry*, 2nd ed., p.296, Macmillan Press, London.

Kameyko, V.A. (1939) 'Compressional strength of brickwork with indirect mesh reinforcement', in Onishchik, L.I. (Ed.): *Experimental Studies of Masonry Structures*, pp.65–89, Center for Scientific Research in Industrial Facilities, Moscow.

Kameyko, V.A. (1949) in Onishchik, L.I. (Ed.): *Experimental Study of Strength of Reinforced Brick Pillars*, pp.157–190, Center for Scientific Research in Industrial Facilities, Moscow.

Kameyko, V.A. (1950) in Onishchik, L.I. (Ed.): *Research of Strength and Deformations of Reinforced Masonry Sections*, pp.123–152, Center for Scientific Research in Industrial Facilities, Moscow.

Karpenko, N.I., Karpenko, S.N. and Eryshev, V.A. (2016) 'Computational dependences for the rebar deformation diagram with a physical yield site', *Technology of Textile Industry*, No. 5, pp.206–210.

Kaushik, H.B., Rai, D.C. and Jain, S.K. (2007a) 'Stress-strain characteristics of clay brick masonry under uniaxial compression', *Journal of Materials in Civil Engineering*, Vol. 19, No. 9, pp.728–739.

Kaushik, H.B., Rai, D.C. and Jain, S.K. (2007b) 'Uniaxial compressive stress-strain model for clay brick masonry', *Current Science*, Vol. 92, No. 4, pp.497–501.

Lazovsky, D.N. and Khatkevich, A.M. (2019) 'Effect of the type of mesh for cross-reinforcement in horizontal mortar seams on the stress-strain state of short, reinforced masonry elements', *Applied Sciences*, Vol. 8, pp.93–100, Vestnik of Polotsk State University, Series F, Constructions, Novopolotsk, Belarus.

Madatyan, S.A. (2000) *Reinforced Concrete Structures*, Voentechlit, Moscow, 256p.

Manual for the Design of Masonry and Reinforced Masonry Structures (to SNiP II-22-81) (1989) *Stone and Reinforced Masonry Structures. Design Standards*, TsNIISK named after Kucherenko of the USSR State Construction Committee, M.: CITO Gosstroy USSR, 152p.

Mohamad, G., Lourenço, P.B. and Roman, H.R. (2007) 'Mechanics of hollow concrete block masonry prisms under compression: review and prospects', *Cement and Concrete Composites*, Vol. 29, No. 3, pp.181–192.

Mohammad, B. et al. (2015) 'Simplified micro modeling of partially grouted masonry assemblages', *Construction and Building Materials*, Vol. 83, pp.159–173, DOI:10.1016 /j.conbuildmat.2015.03.021.

Mohammad, G., Lourenço, P.B. and Roman, H.R. (2007) 'Mechanics of hollow concrete block masonry prisms under compression: Review and prospects', *Cement and Concrete Composites*, Vol. 29, No. 3, pp.181–192.

Mohammad, G., Lourenço, P.B., Roman, H.R., Barbosa, C. and Rizzatti, E. (2012) 'Stress-strain behavior of concrete block masonry prisms under compression', *15th International Brick and Block Masonry Conference*, UFSC, Brazil [online] http://www.hms.civil.uminho.pt/ibmac/2012/4C5.pdf (accessed 11 March 2020).

Pildish, M.Y. and Polyakov, S.V. (1955) *Masonry and Reinforced Masonry Structures of Buildings*, 2nd ed., p.400, State Publishing House on Building and Architecture, Moscow.

PN-70/B-12016 (1970) *Building Ceramics Products*, Technical research, PKN, Warsaw.

PN-71/B-04500 (1971) *Mortars, Studies of Physical and Endurance Characteristics*, PKN, Warsaw.

PN-91/H-04310 (1991) *Static Tensile Test of Metals*, PKN, Warsaw.

PN-EN 1015-11 (2001) *Test Methods for Mortars for Masonry. Part 11: Determination of the Bending and Compressive Strength of Hardened Mortar*, PKN, Warsaw.

PN-EN 772-1 (2003) *Test Methods for Masonry Elements. Part 1: Determination of Compressive Strength*, PKN, Warsaw.

Polyakov, S.V. et al. (1973) *Stone Masonry from Sawn Limestone*, Cartia Moldovanesca, Kishinev, 344p.

Reinforcing Steel (2011) Tensile Test Methods: GOST 12004-81. Replacing GOST 12004-66; Enter, RB 17.12.92, Institute of Standardization and Certification, Minsk: Gos., 10p.

Sousa, R., Guedes, J. and Sousa, H. (2015) 'Characterization of the uniaxial compression behavior of unreinforced masonry – sensitivity analysis based on a numerical and experimental approach', *Architecture of Civil and Mechanical Engineering*, Vol. 15, No. 2, pp.532–547, DOI:10.1016/j.acme.2014.06.007.

SP 5.03.01-2020 (2022) *Concrete And Reinforced Concrete Structures; Introduced on 16.09.2020*, Ministry of Architecture and Construction of the Republic of Belarus, Minsk, 236p.

Stavridis, A. and Shing, P.B. (2010) 'Finite-element modeling of nonlinear behavior of masonry-infilled RC frames', *Journal of Structural Engineering*, Vol. 136, No. 3, pp.285–296.

Stone and Reinforced Masonry Structures (2012) Updated version of SNiP P-22-81*, SP 15.13330.2012. - Enter. 01.01.13. – M., 74p.

Stone and Reinforced Masonry Structures (2018) *Building Design Codes = Stone and Reinforced Stone Structures. Future Norms of Practice*, TKP 45-5.02-308-2017 (33020) – Repl. SNiP II-22-81; Publ. 01.01.18. – Minsk: Ministry of Construction and Architecture, VIII, 111p.

Stone and Reinforced Masonry Structures (2021) *Building Regulations of the Republic of Belarus = stone and reinforced structures. Future norms of practice*, SP 5.02.01-2021, Replacing SSP 45-5.02-308-2017 (33020)); Enter. 01.04.2021, Ministry of Construction Architecture, Minsk, 116p.

Sun, X., Wang, S., Jin, J. et al. (2023) 'Computational methods of mass transport in concrete under stress and crack conditions: a review', *Journal of Intelligent Construction*, Vol. 1, No. 2, 9180015, https://doi.org/10.26599/JIC.2023.9180015.

Wall Materials (1985) *Methods for Determining Ultimate Compressive and Flexural Strength: GOST 8462-85*, Vol. 8, Replacing GOST 8462-75; Enter. USSR 01.07.85. M. Publishing house of standards.

Wang, Z., Gong, F. and Maekawa, K. (2023) 'Multi-scale and multi-chemo – physics lifecycle evaluation of structural concrete under environmental and mechanical impacts', *Journal of Intelligent Construction*, Vol. 1, No. 1, p.9180003, https://doi.org/10.26599/JIC.2023.9180003.

Yaremenko, E.A. and Yaremenko, N.A. (2016) 'Diagrams of concrete deformation and masonry', *Vestnik of Odesa State Academy of Construction and Architecture*, No. 63, pp.103–109.